Letter

Hyperfine interaction limits polarization entanglement of photons from semiconductor quantum dots

Christian Schimpf[1,*] Francesco Basso Basset[2] Maximilian Aigner[1] Wolfgang Attenender[1] Laia Ginés[3] Gabriel Undeutsch[1] Marcus Reindl[1] Daniel Huber[1] Dorian Gangloff[4] Evgeny A. Chekhovich[5] Christian Schneider[6] Sven Höfling[7] Ana Predojević[3] Rinaldo Trotta[2] and Armando Rastelli[1]

[1]Institute of Semiconductor and Solid State Physics, Johannes Kepler University Linz, 4040 Linz, Austria
[2]Department of Physics, Sapienza University of Rome, 00185 Rome, Italy
[3]Department of Physics, Stockholm University, 106 91 Stockholm, Sweden
[4]Department of Engineering Science, University of Oxford, Oxford OX1 3PJ, United Kingdom
[5]Department of Physics and Astronomy, University of Sheffield, Sheffield S3 7RH, United Kingdom
[6]Institute of Physics, Carl von Ossietzky Universität Oldenburg, 26111 Oldenburg, Germany
[7]Julius-Maximilians-Universität Würzburg, Physikalisches Institut, Lehrstuhl für Technische Physik, Am Hubland, 97074 Würzburg, Germany

(Received 18 February 2023; revised 27 April 2023; accepted 17 July 2023; published 15 August 2023)

Excitons in quantum dots are excellent sources of polarization-entangled photon pairs, but a quantitative understanding of their interaction with the nuclear spin bath is still missing. Here we investigate the role of hyperfine energy shifts using experimentally accessible parameters and derive an upper limit to the achievable entanglement fidelity. Our results are consistent with all available literature, indicate that spin noise is often the dominant process limiting the entanglement in InGaAs quantum dots, and suggest routes to alleviate its effect.

DOI: 10.1103/PhysRevB.108.L081405

Semiconductor quantum dots (QDs) have emerged as outstanding sources of single photons [1,2] and photon pairs [3,4] for potential applications in quantum communication and information processing. Most of the proofs of principle demonstrations in these areas have relied on In(Ga)As QDs obtained via the Stranski-Krastanow (SK) epitaxial growth [5] on GaAs substrates. A key advantage of QDs over other solid-state quantum emitters is their capability of emitting polarization-entangled photon pairs using the biexciton-exciton (XX-X) decay cascade [6–8] (see inset of Fig. 1). However, in spite of many careful investigations on SK and most of the other QD types [7–17], entanglement fidelity values above 0.9 could so far only be achieved by resorting to lossy time-filtering techniques [18–20]. In contrast, fidelity values of up to 0.98 [21] have been reported for GaAs QDs obtained via local Al-droplet etching (LDE) on AlGaAs [22–24]. The origin of this large discrepancy is still unclear and solving this puzzle would enhance the understanding of the physics of QDs and guide the improvement of the QD performance as sources of entangled photons.

Several potential dephasing and mixing channels have been identified that could limit the polarization entanglement in QDs. Electron-hole exchange interaction causes the well-studied fine-structure-splitting (FSS) between the bright X levels [25] in QDs with in-plane asymmetry. Other possible limitations are spin scattering [26], phonon-induced dephasing [27,28], laser-induced AC-Stark shifts [29] and their combination [30]. Nuclear spin noise due to stochastic hyperfine shifts, known as Overhauser fluctuations [31–33], have been proposed as the probable dominant dephasing mechanism in In(Ga)As QDs, motivated by the high nuclear spin (9/2) of In [34–36] compared to Ga and As (3/2), but the weight of nuclear spin noise has not been quantified so far.

Here we investigate the polarization entanglement of photon pairs generated by state-of-the-art InGaAs QDs [37,38] with radiative lifetimes $T_1 < 500$ ps and a very small FSS ranging from $\lesssim 0.4$ to ~ 2.4 μeV. We provide a quantitative estimate of the upper limit of the entanglement degree achievable with such QDs due to nuclear spin noise and show that this limit is fully consistent with our measurements as well as former experimental results [4,13,14,26,39], including those resorting to time-filtering [15,17–20] and Purcell enhancement [4]. Our numerical results are based on direct measurements of the nuclear hyperfine noise on the ground-state electron in InGaAs QDs, which reveal an inhomogeneous electron-spin coherence time $T_2^* \simeq 1.7$ ns [32,40,41]. We further show that the consistently higher degree of entanglement found in LDE GaAs QDs [21,35,36] can be tracked back to the lower T_1 ($\sim$230 ps) and the simultaneously higher measured electron spin T_2^* ($\sim$2.6 ns [42]).

The energy levels relevant for generating entangled photons from QDs are sketched in Fig. 1. The level structure of the neutral exciton states (X) is primarily defined by the electron-hole exchange interaction [25]. An anisotropy of this interaction in the x-y plane, perpendicular to the growth direction z, leads to a FSS between the "bright" (optically

*christian.schimpf@eng.ox.ac.uk

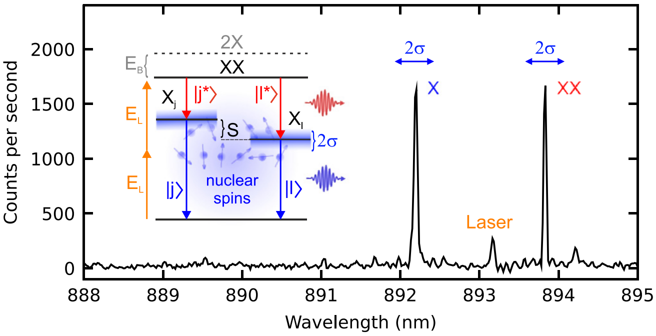

FIG. 1. Spectrum of an InGaAs QD (QD1) under two-photon excitation (TPE). The sketch depicts the biexciton-exciton (XX-X) cascade. TPE is performed by tuning the energy E_L of a pulsed laser to half of the XX energy. Here, the XX level lies $E_B = 2.5$ meV below the energy of two uncorrelated excitons energy (2X). The X states are split by the constant fine-structure splitting S and also by the inhomogeneous Overhauser shift (OS) with a normally distributed amplitude with a standard deviation σ.

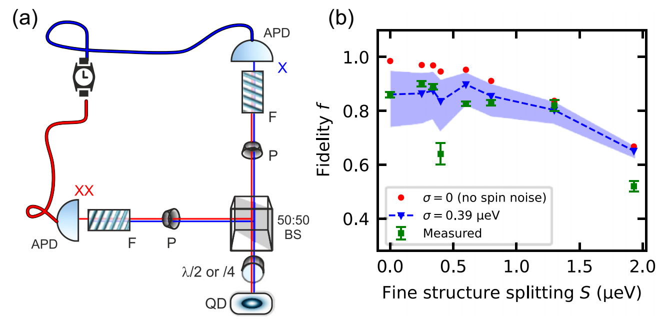

FIG. 2. (a) Setup used to determine the entanglement fidelity of the QD photon source. A 50:50 nonpolarizing beam splitter (BS) is placed directly after the source. Waveplates before and polarizers (P) after the BS set the measurement basis for XX and X. The emitted photons are spectrally filtered (F) before impinging on avalanche photodiodes (APD). (b) Measured fidelity values for different QDs (squares) plotted against the respective FSS values. The red dots show the expected fidelity when only accounting for the FSS and the lifetime, and the blue area depicts the range of expected values when including fluctuating Overhauser shifts according to the values of the electron T_2^* reported in the literature.

dipole-allowed) excitons. In addition to the FSS, the interaction between the exciton and the nuclear spins leads to an Overhauser shift (OS), mediated by the hyperfine interaction, depending on the X spin configuration and nuclear spins' orientations. The biexciton state (XX), as a singlet state, is neither affected by FSS nor by the hyperfine shifts. In the absence of stabilizing Knight fields [32] or externally applied magnetic fields [25,43] the nuclear spins change their orientation and magnitude randomly at timescales in the order of $\tau_S \approx 100\,\mu s$ [31,33]. Consequently, the OS changes many times during entanglement measurements, which take place on typical timescales of seconds, so the OS acts as an inhomogeneous broadening for the X level, following a Gaussian distribution. The standard deviation σ of the OS amplitudes can be identified via their connection to the inhomogeneous spin coherence time T_2^* of the X. The hole's hyperfine contribution is typically at least ten times smaller than the electron's [44], so that the electron spin T_2^* constitutes a good estimate of the X coherence time within about 10%. The expression for σ then reads as [31,40]

$$\sigma \simeq \frac{\hbar}{T_2^*} = \sqrt{\frac{\sum_n x_n A_n^2 I_n (I_n + 1)}{N}}, \qquad (1)$$

with x_n the fraction of the nuclear species n, A_n the hyperfine coupling constant (in the order of $50\,\mu$eV [40]), I_n the nuclear spin, and N the number of nuclei in contact with the electron wave function. The electron spin T_2^* can be determined by measuring its free induction decay via Ramsey interferometry [41,45]. For InGaAs QDs, values of around $T_2^* \simeq 1.7$ ns are typically observed [32,40,41,46], which results in $\sigma \simeq 0.39\,\mu$eV. From these values, a time-averaged loss of X coherence of approximately $1 - \exp[-(T_1/T_2^*)^2] = 6\%$ [42,45] can be expected, leading to a significant degradation of polarization entanglement. In comparison, for LDE GaAs QDs, with $T_1 \simeq 230$ ps and $T_2^* \simeq 2.6$ ns [42], the loss amounts to $<1\%$, providing already a clear hint on the origin of the discrepancy between the fidelity values observed for SK InGaAs and LDE GaAs QDs.

We now investigate the generation of entangled photon pairs in individual InGaAs QDs at a temperature of 5 K. The SK QDs were partially capped and annealed, resulting in ~2-nm-high QDs with an average In fraction of $x_{In} = 0.45(5)$ [38]. The employed material, from the same wafer as the one used in Ref. [37], is of state-of-the-art quality with high single-photon indistinguishability and an average X lifetime as low as 400 ps. To limit the generation of free carriers in the QD surroundings, we create the XX state via coherent two-photon excitation (TPE) [47], as sketched in the inset of Fig. 1. To maximize the chances of observing entanglement fidelities beyond state of the art, we focus on QDs selected out of a much larger ensemble because of their intrinsically small value S of the FSS (see inset of Fig. 1), which we obtain from polarization-resolved photoluminescence (PL) spectra with an accuracy of about $0.2\,\mu$eV (see Supplemental Material for details [48]). Figure 1 depicts the TPE-PL spectrum from an InGaAs QD (QD1) at π-pulse condition, with $S = 1.3(3)\,\mu$eV and an energy difference between the XX and the X photons of $E_B = 2.4$ meV (1.6 nm). The average radiative lifetimes of about $T_{1,XX} = 150$ ps, $T_{1,X} = 400$ ps observed in this sample are compatible with those observed under resonant excitation in Ref. [37]. In the Supplemental Material [48], we provide details about the excitation and decay dynamics of the measured QDs.

The fidelity of a XX-X two-photon state ρ to the $|\phi^+\rangle$ Bell state is defined as $f := \langle\phi^+|\rho|\phi^+\rangle$. We experimentally obtain f via the setup depicted in Fig. 2(a), in which the emitted state can be projected into arbitrary two-qubit states by rotating the waveplate(s) in front of the beam splitter. Using a coincidence window of 3 ns the $g^{(2)}(0)$ values for XX and X are ~0.015 on average, which is comparable with former reports on similar QDs [13] and indicate negligible multipair emission (see Supplemental Material for details [48]). Figure 2(b) shows the measured f values (squares) as a function of S. In the absence of dephasing mechanisms we would expect a monotonic decrease of the time-averaged f with increasing S, as a finite FSS induces a time-dependent evolution of the entangled state [26] (red dots). However, we find that none of the measured f exceed a value of 0.9 and that reducing S below 1 μeV (close to the natural linewidth of the X transitions) leads to no significant increase in f. These findings, which are in line with previous reports, clearly indicate the presence of dephasing processes.

Considering the relevant properties of the studied QDs (X lifetime of about 400 ps, corresponding to a natural linewidth δ_F of about 1.6 μeV, which is much larger than the minimum value of S) and the excitation dynamics (TPE with pulse lengths of 7 ps, much shorter than the XX lifetime of 200 ps), we conclude that excitation-induced dephasing [29] and re-excitation cannot explain the relatively low f values for $S \lesssim 1$ μeV, as both effects combined would account for less than a 0.01 drop of fidelity. The measurement temperature of 5 K is sufficiently low to exclude significant phonon-induced dephasing [27,28,30], as this would be incompatible with the negligible change of f we observed when varying the temperature from 5 to 20 K for two different QDs (see Supplemental Material [48]). Finally, we can rule out charge noise as a dominant dephasing mechanism, as the two mentioned QDs exhibit very similar f values in spite of significantly different linewidths ($\leqslant 12\delta_F$ and $\approx 44\delta_F$), indicating that the latter QD is subject to pronounced charge noise [33,49]. We therefore ascribe the limited maximum value of entanglement to the interplay of finite FSS and nuclear spin noise, as described by the model we derive in the following.

The typical bright-dark exciton splitting of $\sim$100 μeV [25,32] is much larger than the S and σ of the QDs considered here. Therefore we can describe the X dynamics in the two-dimensional bright exciton subspace in good approximation. In the basis given by $X_{H/V} = \{(|{+1}\rangle \pm |{-1}\rangle)/\sqrt{2}\}$, where $|\pm 1\rangle$ are the eigenstates of the total electron-hole angular momentum along the z direction, the Hamiltonian is then given by [25]

$$H = \begin{pmatrix} \delta_1 & \delta_2 \\ \delta_2^* & -\delta_1 \end{pmatrix}, \tag{2}$$

where $\delta_1 = S/2$ and $\delta_2 = ih_z$, with h_z the OS due to the finite nuclear spin polarization in the QD. In the frozen spin approximation (when $\tau_S \gg T_1$) [31,32] H can be treated as time independent and we can construct the entangled state of the two photons emitted in the XX-X radiative decay cascade for a fixed h_z as

$$|\psi_{h_z}\rangle(t) = \frac{1}{\sqrt{2}}(|j^*\rangle \otimes |j\rangle + e^{-(i/\hbar)\Delta_E t}\,|l^*\rangle \otimes |l\rangle), \tag{3}$$

with t the emission time of the X photon relative to that of the XX photon. The orthonormal eigenstates $|j\rangle$ and $|l\rangle$ of Eq. (2) are defined in the basis of the horizontal $|H\rangle$ and vertical $|V\rangle$ polarization and have an energy difference $\Delta_E = 2\sqrt{\delta_1^2 + \delta_2^2}$. Due to conservation of angular momentum, the XX photon eigenstates are necessarily the complex conjugates (*) of the X photon eigenstates (see Supplemental Material for details [48]). The time evolution of the two-photon density matrix $\rho_{h_z}(t) = |\psi_{h_z}\rangle\langle\psi_{h_z}|$ is then given by

$$i\hbar\frac{d}{dt}\rho_{h_z}(t) = [\mathbb{I}^{(2)} \otimes H, \rho_{h_z}(t)], \tag{4}$$

with $\mathbb{I}^{(2)}$ the 2×2 identity matrix. The differential equation, Eq. (4), can be readily solved numerically. The time-averaged density matrix $\langle\rho\rangle_t$ is calculated by drawing h_z multiple times from a normal distribution with a mean value of zero and a standard deviation of σ. The value of S remains constant. By indicating with k the fraction of events with no more than one photon pair per excitation cycle, we account for the multiphoton emission probability $1-k$ as in [50]:

$$1 - k \approx \frac{g^{(2)}_{XX}(0) + g^{(2)}_{X}(0)}{2}\,\eta_P, \tag{5}$$

with η_P the photon-pair-emission probability per excitation pulse (See Supplemental Material [48] for details). By measuring the quantities in the above equation for each QD, we add a mixing channel to $\langle\rho\rangle_t$ so that

$$\tilde{\rho} = k\,\langle\rho\rangle_t + \frac{1-k}{4}\mathbb{I}^{(4)}, \tag{6}$$

with $\mathbb{I}^{(4)}$ the 4×4 identity matrix. In the Supplemental Material [48] we provide further details about the calculation of $\tilde{\rho}$ and how to derive the fidelity

$$f = \frac{1}{4}\left(1 + k + \frac{2k}{1 + 4T_1^2(S^2 + \sigma^2)/\hbar^2}\right). \tag{7}$$

Previously derived equations take spin noise into account only via a phenomenological spin scattering [26], which acts as a mixing channel. However, the physical origin of such effects had not been sufficiently clarified and no clear connection to measurable quantities had been drawn so far. In contrast, the stochastic energy shift σ in our model manifests as a pure dephasing channel and is a consequence of the random OS directly measured in experiments on electron spins confined in QDs [31,32,41,45,46].

The red dots in Fig. 2(b), which depict the fidelity calculated from Eq. (7) with $\sigma = 0$ and using the measured S, T_1, and k for each individual dot, confirm that in the absence of other mechanisms, f should reach values exceeding 0.98. The blue points correspond instead to the estimation for $\sigma \simeq 0.39$ μeV ($T_2^* \simeq 1.7$ ns [41,46]) and the filled blue area depicts the range of f between the shortest ($T_2^* = 1$ ns [32]) and longest ($T_2^* = 3.2$ ns [45]) coherence times in In(Ga)As QDs reported in the literature. We see that no data point lies above the expectations from the model including the realistic effect of OS. Most importantly, our model reproduces the plateau of f values for $S \lesssim \sigma$ and allows us to ascribe it to the dominant role played by the OS while, for $S \gg \sigma$ the effect of the FSS dominates.

Since the spin properties of InGaAs QDs can vary strongly from QD to QD due to atomistic disorder related to alloying and consequent inhomogeneous strain and piezoelectric fields, it is desirable to measure the FSS-dependent fidelity for one single QD (QD1p). Such measurements have been formerly conducted on InGaAs QDs using magnetic, electric, and/or strain fields [14,26,39,51,52] but only under nonresonant excitation, which may introduce additional

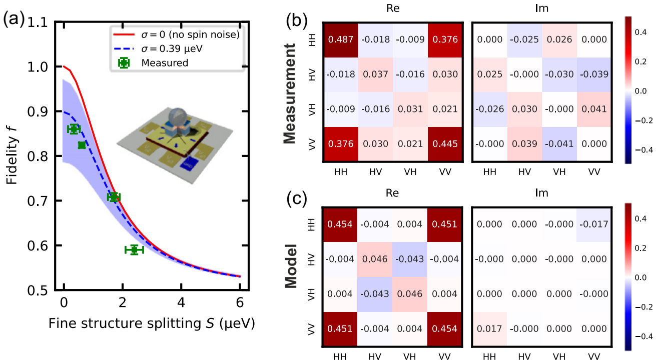

FIG. 3. (a) Measured fidelity values of QD1p as a function of strain-dependent S. The red line shows the expected fidelity for $\sigma = 0$ (no spin noise), and the blue area depicts the expected fidelity range when including OS. The sketch shows the piezoelectric actuator used for tuning S. (b) Real and imaginary parts of the two-qubit density matrix, measured by state tomography on QD1p [$T_1 = 430(4)$ ps, $S = 0.4(2)$ μeV, and $k = 0.990(5)$] with 16 measurement bases, calculated using the maximum-likelihood approach with a resulting fidelity of 0.85(1), a purity of 0.74(2), and a concurrence of 0.69(2). (c) Modeled density matrix for QD1p, assuming $\sigma = 0.41$ μeV ($T_2^* = 1.6$ ns), with a resulting fidelity of 0.89, a purity of 0.81, and a concurrence of 0.79.

entanglement-degrading effects. To eliminate this uncertainty we use TPE and tune S with a piezoelectric strain-tuning actuator [sketched in Fig. 3(a)], similar to the one used to achieve a fidelity of 0.98 [21] in LDE GaAs QDs (see Supplemental Material for details [48]). The green squares in Fig. 3(a) show the measured values of f for different S. The red line shows the expected value of f according to Eq. (7) for $\sigma = 0$. The blue dashed line, just like in the previous measurements, depicts the case for $\sigma = 0.39$ μeV ($T_2^* = 1.7$ ns [41,46]) and the filled blue area depicts the range of f for the range of reported T_2^* values. Again, all f values lie well within the range predicted by Eq. (7), when considering the measured T_1, k, and varied S of QD1p.

To confirm the reliability of our fidelity measurements, which may be affected by polarization-altering effects in the used setup [Fig. 2(a)], we performed a state tomography with 16 measurement bases on QD1p at the lowest value of $S = 0.4(2)$ μeV, obtaining the density matrix ρ_T shown in Fig. 3(b) via the maximum-likelihood estimator [53]. The fidelity calculated from ρ_T is $f = 0.85(1)$, and the purity and the concurrence C [54], which are independent from a unitary rotation of the state, are calculated as 0.74(2) and 0.69(2), respectively. The slightly lower f compared to the 0.89(1) obtained by the fidelity estimation could stem from the additional waveplates required for the state tomography, which are known to induce slight state mixing by the inhomogeneities in the birefringent material. For comparison, the density matrix from Eq. (6) is shown in Fig. 3(c) using the measured values of S, T_1, and k. The value for the electron spin T_2^* was estimated to 1.6 ns ($\sigma = 0.41$ μeV) to match the $f = 0.89$ measured using the fidelity estimation setup.

Before comparing the results of our model with former experimental results we emphasize that our model provides an upper limit for the degree of entanglement which may

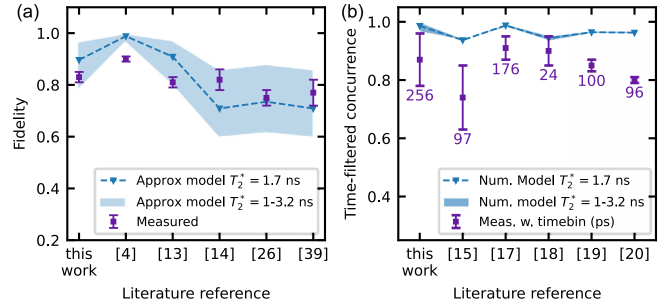

FIG. 4. (a) Measured maximum f from InGaAs QDs with $S \approx 0$ from the indicated references, compared against the values expected from Eq. (7), taking into account the reported T_1. The leftmost data point refers to QD1p. (b) Measured concurrence from the references indicated on the x axis. The measurements are compared against the values calculated by numerically propagating Eq. (4) from 0 up to the used coincidence window (indicated in the graph in picoseconds), taking into account the reported values for T_1 and S. The leftmost data point refers to QD1p at its lowest value of S.

be observed experimentally, given the measured electron spin T_2^* and exciton T_1. Other entanglement-degrading effects may still be present. As an example, the concurrence of 0.79 derived from the density matrix in Fig. 3(c) is higher than the measured 0.69(2) and some entries of the experimentally reconstructed density matrix are not reproduced by the model (e.g., the $\langle HH|\rho|HV\rangle$ component). In addition, one data point in Fig. 2(b), with $f \simeq 0.64$ for an S of only 0.4(2) μeV deviates from the trend obtained from the others and was found to correspond to a QD showing a strong degree of linear polarization of the X signal (see Supplemental Material [48]). This brings us to the conclusion that effects like heavy-hole–light-hole mixing [55–57] or strain-activated quadrupolar double spin flips [32,58,59] could act as non-negligible mixing channels. In fact, state mixing could explain the discrepancy between the expected and the measured concurrence for the QD1p in Fig. 3, while the fidelity matches better. The reason is that the concurrence drops significantly faster compared to the fidelity in the presence of a mixing channel than for pure dephasing channels (see Supplemental Material for details [48]).

In Fig. 4(a) we show a compilation of f values for InGaAs QDs with $S \leqslant 0.4$ μeV from representative work [13,14,26,39], with T_1 ranging from 400 ps to 1 ns and compare them against the range of f predicted by Eq. (7). We see that the values consistently lie inside the range expected from the reported T_2^* as used in Figs. 2 and 3, indicating that OS are probably the dominant source of dephasing in those measurements. In the plot we also show a data point for a QD with $T_1 = 127(1)$ ps and $S \leqslant 1.2$ μeV in a Purcell-enhancing resonator [4], for which excitation-induced dephasing may, however, be appreciable [29]. Finally, Fig. 4(b) shows the values of C from the literature, measured for other QDs with finite S when relying on time filtering [15,17–20]. The emission wavelengths range from 870 to 1550 nm. The data points show the maximum achieved C when including only photons within the coincidence windows stated in the graph. The values are compared against the range calculated numerically from Eq. (4) again using the T_2^* available only for InGaAs

QDs, taking into account the coincidence window, T_1 and S (see Supplemental Material for details [48]). We see that all measured values lie well below the maximum expected for the used coincidence window. The value of C for QD1p (Fig. 3), increases from 0.69(2) to 0.87(9) when decreasing the coincidence window from 3 ns to 256 ps. Propagating Eq. (4) up to the detector resolution of 350 ps, however, results in $C \approx 0.98$, again supporting the presence of additional (possibly time-independent) entanglement-degrading processes requiring further attention.

In summary, we have studied the behavior of the polarization entanglement fidelity on several InGaAs QDs with different FSS and on a single strain-tuned QD on a sample bonded onto a piezoelectric actuator. For the latter, full state tomography was performed for the lowest achieved FSS to quantify the purity and the concurrence of the entangled state. The results are in good agreement with a theoretical model, which predicts an upper limit for the observable fidelity using the measured FSS of the exciton (X), its radiative lifetime, the multiphoton-pair emission probability, and the inhomogeneous electron coherence time T_2^* as an input. From the model we conclude that slowly varying random OSs, prominent in QDs with abundant nonzero nuclear spins, lead to a pronounced dephasing of the bright X states over time, which limits the time-averaged polarization entanglement in InGaAs QDs. By comparing the model predictions with our data and values reported in the literature, we find that OSs often constitute the dominant degradation mechanism. This result is consistent with the higher fidelity values of about 0.98 observed in LDE GaAs QDs, mainly due to the lower X lifetimes of about 230 ps [21]. Additionally, the electron spin T_2^* in LDE GaAs QDs was found to be higher ($\approx$2.6 ns) [42], as expected from Eq. (1) when considering the lack of In and the approximately doubled number of nuclei N in contact with the electron [42], compared to InGaAs QDs [41]. Our results are also compatible with previous claims of dephasing-free QD sources of polarization-entangled photon pairs [18,19] in the limit of low detector time jitter <50 ps. The entanglement can be enhanced by lowering the fraction of high-spin materials (like In), while increasing the number of nuclei in contact with the electron wave function and/or decreasing the X lifetime [60]. Alternatively, precooling the nuclear spin bath [41,45] can provide a tuning knob for σ. These measures could boost the polarization entanglement of InGaAs QDs, making them compatible with state-of-the-art quantum communication protocols.

The authors thank S. Moser for his assistance with the optical setup and U. Kainz for the help in device processing. This work has been supported by the Austrian Academy of Sciences (ÖAW), the QuantERA HYPER-U-P-S project, which received funding from the QuantERA ERA-NET Cofund in Quantum Technologies implemented within the European Union's Horizon 2020 research and innovation program and the Austrian Science Fund (FWF) I 3762, the QD-E-QKD project funded within the QuantERA II program that has received funding from the European Union's Horizon 2020 research and innovation program under Grant Agreement No. 101017733; the European Union's Horizon 2020 research and innovation program under Grant Agreements No. 899814 (Qurope) and No. 871130 (ASCENT+); the PNRR MUR project PE0000023-NQSTI (the National Quantum Science and Technology Institute); the FWF FG 5, I 4380, and I 4320; and the Linz Institute of Technology (LIT) and the LIT Secure and Correct Systems Lab funded by the State of Upper Austria. We further acknowledge funding by the DFG within project PR1749/1-1. A.P. would like to acknowledge the support of the Swedish Research Council. L.G. was supported by the Knut and Alice Wallenberg Foundation [through the Wallenberg Centre for Quantum Technology (WACQT)]. D.G. was supported by a University Research Fellowship from the Royal Society. E.A.C. was supported by a University Research Fellowship from the Royal Society and through EPSRC Grant No. EP/V048333/1.

[1] P. Senellart, G. Solomon, and A. White, High-performance semiconductor quantum-dot single-photon sources, Nat. Nanotechnol. **12**, 1026 (2017).

[2] N. Tomm, A. Javadi, N. O. Antoniadis, D. Najer, M. C. Löbl, A. R. Korsch, R. Schott, S. R. Valentin, A. D. Wieck, A. Ludwig, and R. J. Warburton, A bright and fast source of coherent single photons, Nat. Nanotechnol. **16**, 399 (2021).

[3] J. Liu, R. Su, Y. Wei, B. Yao, S. F. Covre da Silva, Y. Yu, J. Iles-Smith, K. Srinivasan, A. Rastelli, J. Li, and X. Wang, A solid-state source of strongly entangled photon pairs with high brightness and indistinguishability, Nat. Nanotechnol. **14**, 586 (2019).

[4] H. Wang, H. Hu, T. H. Chung, J. Qin, X. Yang, J. P. Li, R. Z. Liu, H. S. Zhong, Y. M. He, X. Ding, Y. H. Deng, Q. Dai, Y. H. Huo, S. Höfling, C. Y. Lu, and J. W. Pan, On-Demand Semiconductor Source of Entangled Photons Which Simultaneously Has High Fidelity, Efficiency, and Indistinguishability, Phys. Rev. Lett. **122**, 113602 (2019).

[5] H. Vural, S. L. Portalupi, and P. Michler, Perspective of self-assembled InGaAs quantum-dots for multi-source quantum implementations, Appl. Phys. Lett. **117**, 030501 (2020).

[6] O. Benson, C. Santori, M. Pelton, and Y. Yamamoto, Regulated and Entangled Photons from a Single Quantum Dot, Phys. Rev. Lett. **84**, 2513 (2000).

[7] N. Akopian, N. H. Lindner, E. Poem, Y. Berlatzky, J. Avron, D. Gershoni, B. D. Gerardot, and P. M. Petroff, Entangled Photon Pairs from Semiconductor Quantum Dots, Phys. Rev. Lett. **96**, 130501 (2006).

[8] R. J. Young, R. M. Stevenson, P. Atkinson, K. Cooper, D. A. Ritchie, and A. J. Shields, Improved fidelity of triggered entangled photons from single quantum dots, New J. Phys. **8**, 29 (2006).

[9] R. Hafenbrak, S. M. Ulrich, P. Michler, L. Wang, A. Rastelli, and O. G. Schmidt, Triggered polarization-entangled photon pairs from a single quantum dot up to 30 K, New J. Phys. **9**, 315 (2007).

[10] C. L. Salter, R. M. Stevenson, I. Farrer, C. A. Nicoll, D. A. Ritchie, and A. J. Shields, An entangled-light-emitting diode, Nature (London) **465**, 594 (2010).

[11] A. Dousse, J. Suffczyński, A. Beveratos, O. Krebs, A. Lemaître, I. Sagnes, J. Bloch, P. Voisin, and P. Senellart, Ultrabright source of entangled photon pairs, Nature (London) **466**, 217 (2010).

[12] G. Juska, V. Dimastrodonato, L. O. Mereni, A. Gocalinska, and E. Pelucchi, Towards quantum-dot arrays of entangled photon emitters, Nat. Photon. **7**, 527 (2013).

[13] M. Müller, S. Bounouar, K. D. Jöns, M. Glässl, and P. Michler, On-demand generation of indistinguishable polarization-entangled photon pairs, Nat. Photon. **8**, 224 (2014).

[14] R. Trotta, J. S. Wildmann, E. Zallo, O. G. Schmidt, and A. Rastelli, Highly entangled photons from hybrid piezoelectric-semiconductor quantum dot devices, Nano Lett. **14**, 3439 (2014).

[15] F. Olbrich, J. Höschele, M. Müller, J. Kettler, S. Luca Portalupi, M. Paul, M. Jetter, and P. Michler, Polarization-entangled photons from an InGaAs-based quantum dot emitting in the telecom C-band, Appl. Phys. Lett. **111**, 133106 (2017).

[16] T. Müller, J. Skiba-Szymanska, A. B. Krysa, J. Huwer, M. Felle, M. Anderson, R. M. Stevenson, J. Heffernan, D. A. Ritchie, and A. J. Shields, A quantum light-emitting diode for the standard telecom window around 1550 nm, Nat. Commun. **9**, 862 (2018).

[17] K. D. Zeuner, K. D. Jöns, L. Schweickert, C. Reuterskiöld Hedlund, C. Nuñez Lobato, T. Lettner, K. Wang, S. Gyger, E. Schöll, S. Steinhauer, M. Hammar, and V. Zwiller, On-demand generation of entangled photon pairs in the telecom C-band with InAs quantum dots, ACS Photonics **8**, 2337 (2021).

[18] R. Winik, D. Cogan, Y. Don, I. Schwartz, L. Gantz, E. R. Schmidgall, N. Livneh, R. Rapaport, E. Buks, and D. Gershoni, On-demand source of maximally entangled photon pairs using the biexciton-exciton radiative cascade, Phys. Rev. B **95**, 235435 (2017).

[19] A. Fognini, A. Ahmadi, M. Zeeshan, J. T. Fokkens, S. J. Gibson, N. Sherlekar, S. J. Daley, D. Dalacu, P. J. Poole, K. D. Jöns, V. Zwiller, and M. E. Reimer, Dephasing free photon entanglement with a quantum dot, ACS Photonics **6**, 1656 (2019).

[20] M. Anderson, T. Müller, J. Skiba-Szymanska, A. B. Krysa, J. Huwer, R. M. Stevenson, J. Heffernan, D. A. Ritchie, and A. J. Shields, Gigahertz-Clocked Teleportation of Time-Bin Qubits with a Quantum Dot in the Telecommunication *C* Band, Phys. Rev. Appl. **13**, 054052 (2020).

[21] D. Huber, M. Reindl, S. F. Covre da Silva, C. Schimpf, J. Martín-Sánchez, H. Huang, G. Piredda, J. Edlinger, A. Rastelli, and R. Trotta, Strain-Tunable GaAs Quantum Dot: A Nearly Dephasing-Free Source of Entangled Photon Pairs on Demand, Phys. Rev. Lett. **121**, 033902 (2018).

[22] M. Gurioli, Z. Wang, A. Rastelli, T. Kuroda, and S. Sanguinetti, Droplet epitaxy of semiconductor nanostructures for quantum photonic devices, Nat. Mater. **18**, 799 (2019).

[23] S. F. Covre da Silva, G. Undeutsch, B. Lehner, S. Manna, T. M. Krieger, M. Reindl, C. Schimpf, R. Trotta, and A. Rastelli, GaAs quantum dots grown by droplet etching epitaxy as quantum light sources, Appl. Phys. Lett. **119**, 120502 (2021).

[24] L. Zhai, G. N. Nguyen, C. Spinnler, J. Ritzmann, M. C. Löbl, A. D. Wieck, A. Ludwig, A. Javadi, and R. J. Warburton, Quantum interference of identical photons from remote GaAs quantum dots, Nat. Nanotechnol. **17**, 829 (2022).

[25] M. Bayer, G. Ortner, O. Stern, A. Kuther, A. A. Gorbunov, A. Forchel, P. Hawrylak, S. Fafard, K. Hinzer, T. L. Reinecke, S. N. Walck, J. P. Reithmaier, F. Klopf, and F. Schäfer, Fine structure of neutral and charged excitons in self-assembled In(Ga)As/(Al)GaAs quantum dots, Phys. Rev. B **65**, 195315 (2002).

[26] A. J. Hudson, R. M. Stevenson, A. J. Bennett, R. J. Young, C. A. Nicoll, P. Atkinson, K. Cooper, D. A. Ritchie, and A. J. Shields, Coherence of an Entangled Exciton-Photon State, Phys. Rev. Lett. **99**, 266802 (2007).

[27] U. Hohenester, G. Pfanner, and M. Seliger, Phonon-Assisted Decoherence in the Production of Polarization-Entangled Photons in a Single Semiconductor Quantum Dot, Phys. Rev. Lett. **99**, 047402 (2007).

[28] A. Reigue, J. Iles-Smith, F. Lux, L. Monniello, M. Bernard, F. Margaillan, A. Lemaitre, A. Martinez, D. P. S. McCutcheon, J. Mørk, R. Hostein, and V. Voliotis, Probing Electron-Phonon Interaction through Two-Photon Interference in Resonantly Driven Semiconductor Quantum Dots, Phys. Rev. Lett. **118**, 233602 (2017).

[29] T. Seidelmann, C. Schimpf, T. K. Bracht, M. Cosacchi, A. Vagov, A. Rastelli, D. E. Reiter, and V. M. Axt, Two-Photon Excitation Sets Fundamental Limit to Entangled Photon Pair Generation from Quantum Emitters, Phys. Rev. Lett. **129**, 193604 (2022).

[30] T. Seidelmann, T. K. Bracht, B. U. Lehner, C. Schimpf, M. Cosacchi, M. Cygorek, A. Vagov, A. Rastelli, D. E. Reiter, and V. M. Axt, Two-photon excitation with finite pulses unlocks pure dephasing-induced degradation of entangled photons emitted by quantum dots, Phys. Rev. B **107**, 235304 (2023).

[31] I. A. Merkulov, A. L. Efros, and M. Rosen, Electron spin relaxation by nuclei in semiconductor quantum dots, Phys. Rev. B **65**, 205309 (2002).

[32] B. Urbaszek, X. Marie, T. Amand, O. Krebs, P. Voisin, P. Malentinsky, A. Högele, and A. Imamoglu, Nuclear spin physics in quantum dots: An optical investigation, Rev. Mod. Phys. **85**, 79 (2013).

[33] A. V. Kuhlmann, J. Houel, A. Ludwig, L. Greuter, D. Reuter, A. D. Wieck, M. Poggio, and R. J. Warburton, Charge noise and spin noise in a semiconductor quantum device, Nat. Phys. **9**, 570 (2013).

[34] T. Kuroda, T. Mano, N. Ha, H. Nakajima, H. Kumano, B. Urbaszek, M. Jo, M. Abbarchi, Y. Sakuma, K. Sakoda, I. Suemune, X. Marie, and T. Amand, Symmetric quantum dots as efficient sources of highly entangled photons: Violation of Bell's inequality without spectral and temporal filtering, Phys. Rev. B **88**, 041306(R) (2013).

[35] D. Huber, M. Reindl, Y. Huo, H. Huang, J. S. Wildmann, O. G. Schmidt, A. Rastelli, and R. Trotta, Highly indistinguishable and strongly entangled photons from symmetric GaAs quantum dots, Nat. Commun. **8**, 15506 (2017).

[36] R. Keil, M. Zopf, Y. Chen, B. Höfer, J. Zhang, F. Ding, and O. G. Schmidt, Solid-state ensemble of highly entangled photon sources at rubidium atomic transitions, Nat. Commun. **8**, 15501 (2017).

[37] Y. M. He, Y. He, Y. J. Wei, D. Wu, M. Atatüre, C. Schneider, S. Höfling, M. Kamp, C. Y. Lu, and J. W. Pan, On-demand semiconductor single-photon source with near-unity indistinguishability, Nat. Nanotechnol. **8**, 213 (2013).

[38] T. Braun, S. Betzold, N. Lundt, M. Kamp, S. Höfling, and C. Schneider, Impact of ex situ rapid thermal annealing on magneto-optical properties and oscillator strength of In(Ga)As quantum dots, Phys. Rev. B **93**, 155307 (2016).

[39] J. Zhang, J. S. Wildmann, F. Ding, R. Trotta, Y. Huo, E. Zallo, D. Huber, A. Rastelli, and O. G. Schmidt, High yield and ultrafast sources of electrically triggered entangled-photon pairs based on strain-tunable quantum dots, Nat. Commun. **6**, 10067 (2015).

[40] R. Stockill, C. Le Gall, C. Matthiesen, L. Huthmacher, E. Clarke, M. Hugues, and M. Atatüre, Quantum dot spin coherence governed by a strained nuclear environment, Nat. Commun. **7**, 12745 (2016).

[41] D. A. Gangloff, G. Éthier-Majcher, C. Lang, E. V. Denning, J. H. Bodey, D. M. Jackson, E. Clarke, M. Hugues, C. Le Gall, and M. Atatüre, Quantum interface of an electron and a nuclear ensemble, Science **364**, 62 (2019).

[42] L. Zaporski, N. Shofer, J. H. Bodey, S. Manna, G. Gillard, M. H. Appel, C. Schimpf, S. F. Covre da Silva, J. Jarman, G. Delamare, G. Park, U. Haeusler, E. A. Chekhovich, A. Rastelli, D. A. Gangloff, M. Atatüre, and C. Le Gall, Ideal refocusing of an optically active spin qubit under strong hyperfine interactions, Nat. Nanotechnol. **18**, 257 (2023).

[43] E. Welander, J. Hildmann, and G. Burkard, Influence of hyperfine interaction on the entanglement of photons generated by biexciton recombination, arXiv:1409.6521.

[44] B. Eble, C. Testelin, P. Desfonds, F. Bernardot, A. Balocchi, T. Amand, A. Miard, A. Lemaître, X. Marie, and M. Chamarro, Hole–Nuclear Spin Interaction in Quantum Dots, Phys. Rev. Lett. **102**, 146601 (2009).

[45] G. Éthier-Majcher, D. Gangloff, R. Stockill, E. Clarke, M. Hugues, C. Le Gall, and M. Atatüre, Improving a Solid-State Qubit through an Engineered Mesoscopic Environment, Phys. Rev. Lett. **119**, 130503 (2017).

[46] D. Press, K. De Greve, P. L. McMahon, T. D. Ladd, B. Friess, C. Schneider, M. Kamp, S. Höfling, A. Forchel, and Y. Yamamoto, Ultrafast optical spin echo in a single quantum dot, Nat. Photon. **4**, 367 (2010).

[47] S. Stufler, P. Machnikowski, P. Ester, M. Bichler, V. M. Axt, T. Kuhn, and A. Zrenner, Two-photon Rabi oscillations in a single $In_xGa_{1-x}As$/GaAs quantum dot, Phys. Rev. B **73**, 125304 (2006).

[48] See Supplemental Material at http://link.aps.org/supplemental/10.1103/PhysRevB.108.L081405 for details about the modeling of the entangled two-photon states, the used QD samples and devices, the experimental methods used to acquire the measured data, the temperature and charge-noise dependence of the measurements, and for a list of relevant parameters of each QD included in this work. It also contains Ref. [61].

[49] C. Schimpf, M. Reindl, P. Klenovský, T. Fromherz, S. F. Covre da Silva, J. Hofer, C. Schneider, S. Höfling, R. Trotta, and A. Rastelli, Resolving the temporal evolution of line broadening in single quantum emitters, Opt. Express **27**, 35290 (2019).

[50] J. Neuwirth, F. Basso Basset, M. B. Rota, J.-G. Hartel, M. Sartison, S. F. Covre da Silva, K. D. Jöns, A. Rastelli, and R. Trotta, A multipair-free source of entangled photons in the solid state, Phys. Rev. B **106**, L241402 (2022).

[51] A. Bennett, Y. M. Pooley, N. R. Stevenson, M. Ward, R. Patel, A. B. de La Giroday, N. Sköld, I. Farrer, C. Nicoll, D. Ritchie *et al.*, Electric-field-induced coherent coupling of the exciton states in a single quantum dot, Nat. Phys. **6**, 947 (2010).

[52] T. Lettner, S. Gyger, K. D. Zeuner, L. Schweickert, S. Steinhauer, C. Reuterskiöld Hedlund, S. Stroj, A. Rastelli, M. Hammar, R. Trotta, K. D. Jöns, and V. Zwiller, Strain-controlled quantum dot fine structure for entangled photon generation at 1550 nm, Nano Lett. **21**, 10501 (2021).

[53] D. F. V. James, P. G. Kwiat, W. J. Munro, and A. G. White, Measurement of qubits, Phys. Rev. A **64**, 052312 (2001).

[54] W. K. Wootters, Entanglement of Formation of an Arbitrary State of Two Qubits, Phys. Rev. Lett. **80**, 2245 (1998).

[55] T. Belhadj, T. Amand, A. Kunold, C. M. Simon, T. Kuroda, M. Abbarchi, T. Mano, K. Sakoda, S. Kunz, X. Marie, and B. Urbaszek, Impact of heavy hole-light hole coupling on optical selection rules in GaAs quantum dots, Appl. Phys. Lett. **97**, 051111 (2010).

[56] C. Tonin, R. Hostein, V. Voliotis, R. Grousson, A. Lemaitre, and A. Martinez, Polarization properties of excitonic qubits in single self-assembled quantum dots, Phys. Rev. B **85**, 155303 (2012).

[57] J. D. Plumhof, R. Trotta, V. Křápek, E. Zallo, P. Atkinson, S. Kumar, A. Rastelli, and O. G. Schmidt, Tuning of the valence band mixing of excitons confined in GaAs/AlGaAs quantum dots via piezoelectric-induced anisotropic strain, Phys. Rev. B **87**, 075311 (2013).

[58] C. Bulutay, Quadrupolar spectra of nuclear spins in strained $In_xGa_{1-x}As$ quantum dots, Phys. Rev. B **85**, 115313 (2012).

[59] E. V. Denning, D. A. Gangloff, M. Atatüre, J. Mørk, and C. Le Gall, Collective Quantum Memory Activated by a Driven Central Spin, Phys. Rev. Lett. **123**, 140502 (2019).

[60] D. Huber, B. U. Lehner, D. Csontosová, M. Reindl, S. Schuler, S. F. Covre da Silva, P. Klenovský, and A. Rastelli, Single-particle-picture breakdown in laterally weakly confining GaAs quantum dots, Phys. Rev. B **100**, 235425 (2019).

[61] L. Wang, A. Rastelli, and O. G. Schmidt, Structural and optical properties of In(Ga)As/GaAs quantum dots treated by partial capping and annealing, J. Appl. Phys. **100**, 064313 (2006).